

Electric field effect in heat transfer in 2D devices

A.I.Volokitin^{1,2*} and B.N.J.Persson²

¹*Samara State Technical University, Molodogvardeiskaya Str.244, 443100 Samara, Russia and*

²*Peter Grünberg Institut, Forschungszentrum Jülich, D-52425, Germany*

We calculate heat transfer between a 2D sheet (e.g. graphene) and a dielectric in presence of a gate voltage. The gate potential induces surface charge densities on the sheet and dielectric, which results in electric field, which is coupled to the surface displacements and, as a consequence, resulting an additional contributions to the radiative heat transfer. The electrostatic and van der Waals interactions between the surface displacement result in the phonon heat transfer, which we calculate taking into account the nonlocality of these interactions. Numerical calculations are presented for heat transfer between graphene and a SiO₂ substrate.

PACS: 42.50.Lc, 12.20.Ds, 78.67.-n

I. INTRODUCTION

The ability to control the electrical properties of materials underlies modern electronics. Currently, in connection with the development of new technologies related to nanoscale thermal management, energy storage and conversion, and information processing, the problem of the management of the heat transfer is being actively considered. The problem of heat transfer is, for example, important in the development of a graphene transistor. Heat generation during high-density electric current flowing in graphene will increase the temperature, which can damage the device. Therefore, it is important to be able to control heat flux.

In 2006, Li *et. al.*¹ proposed a thermal analogue of the field effect transistor for controlling heat transfer by phonons through solid segments, paving the way for creating blocks for processing information^{2,3} using heat flow instead of electric current. More recently the concept of thermal transistor has been expanded to noncontact systems out of thermal equilibrium⁴. In this case, heat fluxes are associated with the transmission of thermal photons from one material to another.

A radiation heat transistor consists of three elements, which by analogy with its electronic counterpart, are called source, drain and gate. Source and drain are maintained at different temperatures to create a temperature gradient. Source, being traditionally hotter than drain, emits thermal photons that transmit heat to the drain. These two solids are separated by intermediate layer made of insulator-metal phase transition material⁵. This layer acts as a gate. By adjusting the gate temperature near a critical value, it is possible radically change the heat flow obtained by drain and even enhance this flow. The device can work either at large separation (far field⁶), where heat fluxes are associated with the propagating photons, or at short distances (near field⁴), where heat is transmitted primarily by photon tunneling. Beyond modulation and heat flow amplification, these structures based on phase transition materials can be used for storage thermal energy and logical operations with thermal photons.

In this article we consider the possibility of controlling the radiative and phonon heat flux between a 2D sheet (e.g. graphene) and a dielectric substrate (e.g. SiO₂) using the field effect, similar to how it is used to control electronic properties in a graphene transistor⁷. The gate voltage induces surface charge densities on the sheet and dielectric. The thermal fluctuations of the displacements of the charged surfaces give rise to an additional contribution to the fluctuating electromagnetic field which result in an additional contributions to the radiative heat transfer. The electrostatic and van der Waals interactions between surface displacements produce the phonon heat transfer. In contrast to our previous “spring” model⁸, now we take into account the nonlocality in these interactions. The methodological approach that is used in this article was previously used to calculate heat transfer between 3D metals⁹. The electrostatic and van der Waals phonon heat transfer was also recently studied in Ref.¹⁰ using different approach.

II. THEORY

A. Radiative heat transfer

Consider a 2D sheet (e.g. graphene) located in the (x, y) -plane at $z = 0$ and separated from a dielectric slab with thickness h (e.g. SiO₂) by vacuum gap with thickness d . The application of the gate voltage (V_G) induces a surface charge density on the sheet, $\sigma_g = ne = E_0/4\pi$, where n is the concentration of the free charge carries in the sheet, E_0 is the electric field in the vacuum gap between the sheet and dielectric. In general, the application of a gate voltage

(V_G) creates an electrostatic potential difference φ between the graphene and the gate electrode, and the addition of charge carriers leads to a shift in the Fermi level (E_F). Therefore V_G is given by¹¹

$$V_G = \frac{E_F}{e} + \varphi \quad (1)$$

with E_F/e being determined by the chemical (quantum) capacitance of the graphene, and φ being determined by the geometrical capacitance C_G . In this article we consider the back gate for which¹¹ $V_{BG} \approx \varphi$, where $\varphi = ne/C_G$ is an electrostatic potential difference between the sheet and the gating electrode where $C_G = \varepsilon_d(0)/4\pi h$, $\varepsilon_d(0)$ is the dielectric constant of the dielectric. The approach which is used in this article can also be applied for the top gate. The radiative heat transfer is associated with the fluctuating electromagnetic field created by thermal fluctuations of the charge and current densities inside the bodies. In the case of a charged surface, thermal fluctuations of the surface displacement will also contribute to the fluctuating electromagnetic field and radiative heat transfer. The heat flux between two surfaces separated by a vacuum gap d , due to evanescent (non-radiative) electromagnetic waves (for which $q > \omega/c$) is determined by the formula¹²⁻¹⁴

$$J^{rad} = \int_0^\infty \frac{d\omega}{2\pi} [\Pi_g(\omega) - \Pi_d(\omega)] \int \frac{d^2q}{(2\pi)^2} \frac{4\text{Im}R_d(\omega)\text{Im}R_g(\omega)e^{-2qd}}{|1 - e^{-2qd}R_d(\omega)R_g(\omega)|^2}, \quad (2)$$

$$\Pi_{g(d)}(\omega) = \frac{\hbar\omega}{e^{\hbar\omega/k_B T g(d)} - 1},$$

$R_{g(d)}$ is the reflection amplitudes for the sheet (dielectric) for p -polarized electromagnetic waves.

To find the reflection amplitude for the charged sheet, write the electric field of the p -polarized electromagnetic wave in the non-retarded limit in the form:

$$\mathbf{E}(\mathbf{q}, \omega, z) = e^{i\mathbf{q}\cdot\mathbf{x} - i\omega t} \times \begin{cases} \mathbf{n}^+ e^{-qz} + R_p n^- e^{qz} \mathbf{n}^-, & z < 0 \\ T \mathbf{n}^+ e^{-qz}, & z > 0 \end{cases} \quad (3)$$

where $\mathbf{x} = (x, y)$, \mathbf{q} is the wave vector in the (x, y) -plane, $\mathbf{n}^\pm = (\mp i\hat{q}, \hat{z})$. The electric field of the electromagnetic wave induces in the sheet the polarization

$$\mathbf{p}(\mathbf{x}, z) = (p_q \hat{q} + p_z \hat{z}) \delta(z) e^{i\mathbf{q}\cdot\mathbf{x} - i\omega t} \quad (4)$$

where p_q and p_z are the parallel and normal components of the surface dipole moment. The boundary condition for the normal component of the electric field can be obtained from the Maxwell equation

$$\nabla \cdot \mathbf{E} = \frac{dE_z}{dz} + iqE_q = -4\pi p_z \delta'(z) - iqp_q \delta(z). \quad (5)$$

Integrating (5) from -0 to $+0$, we get

$$E_z(z = +0) - E_z(z = -0) = -4\pi iqp_q, \quad (6)$$

To obtain the boundary condition for the component of the electric field parallel to the surface, we calculate the circulation of \mathbf{E} around the contour of the rectangle, two sides of which are parallel to the surface and located at $z = \pm 0$, and the other two sides are perpendicular to the surface. The magnetic induction field is continuous on the surface, so the magnetic flux through the area of the rectangle will be zero. Then from the Faraday's law it follows that^{9,15}

$$E_q(z = +0) - E_q(z = -0) = iq \int_{-0}^{+0} dz E_z(z) = -iq \int_{-0}^{+0} dz z \frac{dE_z}{dz} = -4\pi iqp_z. \quad (7)$$

The electromagnetic wave will create mechanical stress on the sheet $\tilde{\sigma}_{zi} = \sigma_{zi}(z = +0) - \sigma_{zi}(z = -0)$, where $\sigma_{zi}(z = \pm 0)$ is the Maxwell stress tensor at $z = \pm 0$, which in electrostatic limit has the form

$$\sigma_{ij} = \frac{1}{4\pi} \left(\tilde{E}_i \tilde{E}_j - \frac{1}{2} \delta_{ij} \tilde{\mathbf{E}} \cdot \tilde{\mathbf{E}} \right), \quad (8)$$

where

$$\tilde{\mathbf{E}} = \mathbf{E} + \hat{z} \begin{cases} E'_0, & z > 0 \\ -E'_0, & z < 0 \end{cases} \quad (9)$$

where $E'_0 = E_0/2 = 2\pi\sigma_g$ is the static electric field created by the surface charge density $\sigma_g = en$ on the sheet, \mathbf{E} is the electric field of the electromagnetic wave, which is determined by (3). To linear order in the amplitude of the electromagnetic wave, the perpendicular component of the stress is determined by

$$\tilde{\sigma}_{zz} \approx \sigma_g \frac{E_z(+0) + E_z(-0)}{2}, \quad (10)$$

where $E_{z(q)}^\pm = E_{z(q)}(z = \pm 0)$. The stress $\tilde{\sigma}_{zz}$ produces a polarization of the sheet, with normal component of the dipole moment

$$p_z = \sigma_g u_z = \sigma_g^2 M_g \frac{E_z(+0) + E_z(-0)}{2}, \quad (11)$$

where M_g is the mechanical susceptibility of the sheet which determines the surface displacement of the sheet under an action of the stress $\tilde{\sigma}_{zz}$: $u_z = M_g \tilde{\sigma}_{zz}$. The stress $\tilde{\sigma}_{zq}$, which produces the polarization parallel to the surface of the sheet, is

$$\tilde{\sigma}_{zq} \approx ne \frac{E_q^+ + E_q^-}{2} \quad (12)$$

Thus, the polarization of graphene parallel to the surface arises due to the effective electric field $E_{\parallel}^{\text{eff}} = (E_q^+ + E_q^-)/2$, which induces the sheet dipole moment $p_q = i\sigma(E_q^+ + E_q^-)/2\omega$ parallel to the surface, where σ is the sheet conductivity. The sheet conductivity can be expressed in terms of the dielectric function $\varepsilon_g = 1 + 2\pi iq\sigma/\omega$. From (3), (6) and (7), the boundary conditions can be written as

$$T - 1 - R = -(\varepsilon_g - 1)(T + 1 - R), \quad (13)$$

$$T - 1 + R = 2\pi q\sigma_g^2 M_g (T + 1 + R), \quad (14)$$

From (13) and (14) follows

$$R_g = \frac{\varepsilon_g - 1 + 2\pi q\sigma_g^2 M_g}{\varepsilon_g(1 - 2\pi q\sigma_g^2 M_g)}. \quad (15)$$

The reflection amplitude (15) has the resonances at $\text{Re}\varepsilon_g = 0$ and $1 - 2\pi q\sigma_g^2 \text{Re}M_g = 0$ associated with the plasmon and phonon polaritons of the sheet, respectively. Close to the phonon polariton resonance

$$R_g \approx \frac{1}{1 - 2\pi q\sigma_g^2 M_g}. \quad (16)$$

Thus in this case the reflection amplitude depends only on M_g and does not depend on ε_g what means that at the phonon polariton resonance the optical properties of the sheet are determined only by the mechanical properties of the flexural mode. The reflection amplitude for the charged dielectric surface can be calculated in the same way as above for the sheet. Neglecting the polarization parallel to the surface, the boundary conditions on the surface of the dielectric can be written as

$$E_z(z = -d + 0) = \varepsilon_d(\omega)E_z(z = -d - 0), \quad (17)$$

$$E_q(z = -d + 0) - E_q(z = -d - 0) = -4\pi i q p_z^d, \quad (18)$$

where $\mathbf{E}(z > -d)$ determines the incident and reflected wave, and $\mathbf{E}(z < -d)$ is the refracted wave. For a constant electric field, the surface density of the polarization charge for the dielectric

$$\sigma_d = -\frac{\varepsilon_d(0) - 1}{\varepsilon_d(0)}\sigma_g, \quad (19)$$

where $\varepsilon_d(\omega)$ is the dielectric function of a substrate, and $p_z^d = \sigma_d M_d E_z(d = -d + 0)$ is the dipole moment normal to the surface. From (17) (18) the reflection amplitude for a charged dielectric surface is

$$R_d = \frac{\varepsilon_d - 1 + 4\pi q\sigma_d^2 M_d \varepsilon_d}{\varepsilon_d + 1 - 4\pi q\sigma_d^2 M_d \varepsilon_d}. \quad (20)$$

For metals $\sigma_g = -\sigma_d$, and in this case (20) is reduced to formula obtained in Ref.⁹. The reflection amplitude has resonance at

$$\text{Re}[\varepsilon_d(1 - 4\pi q\sigma_d^2 M_d)] + 1 = 0. \quad (21)$$

For a polar dielectric, this resonance is associated with surface phonon polaritons arising from the hybridization of optical and acoustic waves. For small potential difference, when $2\pi q\sigma_g^2 M_g \ll 1$ and $4\pi q\sigma_d^2 M_d \ll 1$, the reflection amplitudes are determined by well known formulas¹⁴

$$R_g = \frac{\varepsilon_g - 1}{\varepsilon_g}, \quad (22)$$

$$R_d = \frac{\varepsilon_d - 1}{\varepsilon_d + 1}. \quad (23)$$

B. Phonon heat transfer

1. van der Waals interaction between semi-infinite medium and a 2D sheet

In the case of the van der Waals interaction between a semi-infinite dielectric and a 2D sheet, such as graphene, the potential energy can be written as

$$\begin{aligned} U &= C_2 \int d^2 \mathbf{x}_1 \int d^2 \mathbf{x}_2 \int_{-\infty}^{u_d(\mathbf{x}_1)} dz_1 \frac{1}{[(\mathbf{x}_1 - \mathbf{x}_2)^2 + (d + u_g(\mathbf{x}_2) - z_1)^2]^6} \\ &\quad - C_1 \int d^2 \mathbf{x}_1 \int d^2 \mathbf{x}_2 \int_{-\infty}^{u_d(\mathbf{x}_1)} dz_1 \frac{1}{[(\mathbf{x}_1 - \mathbf{x}_2)^2 + (d + u_g(\mathbf{x}_2) - z_1)^2]^3}, \end{aligned} \quad (24)$$

where $u_d(\mathbf{x})$ and $u_g(\mathbf{x})$ are the surface displacements for the dielectric and sheet. Expanding (24) to second order in displacements, we get

$$\begin{aligned} U &= \pi A \left(\frac{C_2}{45d^9} - \frac{C_1}{6d^3} \right) + \pi \left[\int d^2 \mathbf{x}_1 u_d(\mathbf{x}_1) - \int d^2 \mathbf{x}_2 u_g(\mathbf{x}_2) \right] \left(\frac{C_2}{5d^{10}} - \frac{C_1}{2d^4} \right) \\ &\quad + 6d \int d^2 \mathbf{x}_1 \int d^2 \mathbf{x}_2 u_d(\mathbf{x}_1) u_g(\mathbf{x}_2) \left\{ \frac{C_1}{[(\mathbf{x}_1 - \mathbf{x}_2)^2 + d^2]^4} - \frac{2C_2}{[(\mathbf{x}_1 - \mathbf{x}_2)^2 + d^2]^7} \right\} \\ &\quad + \pi \left(\frac{C_2}{d^{11}} - \frac{C_1}{d^5} \right) \left[\int d^2 \mathbf{x}_1 u_d^2(\mathbf{x}_1) + \int d^2 \mathbf{x}_2 u_g^2(\mathbf{x}_2) \right] + \dots, \end{aligned} \quad (25)$$

At the equilibrium distance the linear terms in the displacement vanish. Thus, the equilibrium distance $d_0 = (2C_2/5C_1)^{1/6}$. The stresses that act on surfaces of the dielectric and sheet, when they are displaced, are determined by

$$\sigma_d = -\frac{\delta U}{\delta u_d(\mathbf{x})} = -6dC_1 \int d^2 \mathbf{x}_2 u_g(\mathbf{x}_2) \left\{ \frac{1}{[(\mathbf{x} - \mathbf{x}_2)^2 + d^2]^4} - \frac{5d_0^6}{[(\mathbf{x} - \mathbf{x}_2)^2 + d^2]^7} \right\} - \frac{\pi C_1 u_d(\mathbf{x})}{d^5} \left[5 \left(\frac{d_0}{d} \right)^6 - 2 \right], \quad (26)$$

$$\sigma_g = -\frac{\delta U}{\delta u_g(\mathbf{x})} = -6dC_1 \int d^2 \mathbf{x}_2 u_d(\mathbf{x}_2) \left\{ \frac{1}{[(\mathbf{x} - \mathbf{x}_2)^2 + d^2]^4} - \frac{5d_0^6}{[(\mathbf{x} - \mathbf{x}_2)^2 + d^2]^7} \right\} - \frac{\pi C_1 u_g(\mathbf{x})}{d^5} \left[5 \left(\frac{d_0}{d} \right)^6 - 2 \right]. \quad (27)$$

Using a Fourier transformation

$$u_i(\mathbf{x}) = \int \frac{d^2 \mathbf{q}}{(2\pi)^2} u_i e^{i\mathbf{q} \cdot \mathbf{x}}, \quad (28)$$

we get

$$\sigma_d = au_d - bu_g, \quad (29)$$

$$\sigma_g = au_g - bu_d, \quad (30)$$

where

$$a = \frac{\pi C_1}{d^5} \left[2 - 5 \left(\frac{d_0}{d} \right)^6 \right], \quad (31)$$

$$b = \frac{\pi q^3 C_1}{4d^2} \left[K_3(qd) - \frac{q^3 d_0^6 K_6(qd)}{192d^3} \right], \quad (32)$$

where we have used that

$$\int d^2 \mathbf{x}_1 \frac{u_1(\mathbf{x}_1)}{[(\mathbf{x}_1 - \mathbf{x})^2 + d^2]^{\mu+1}} = \int \frac{d^2 \mathbf{q}}{(2\pi)^2} u_i e^{i\mathbf{q} \cdot \mathbf{x}} G_{\mu+1}(q), \quad (33)$$

$$G_{\mu+1}(q) = \int d^2 \mathbf{x} \frac{e^{i\mathbf{q} \cdot \mathbf{x}}}{(r^2 + d^2)^{\mu+1}} = 2\pi \int_0^\infty \frac{J_0(qr) r dr}{(r^2 + d^2)^{\mu+1}} = \frac{\pi}{2^{\mu-1}} \left(\frac{q}{d} \right)^\mu \frac{K_\mu(qd)}{\Gamma(\mu+1)} \quad (34)$$

where $K_\mu(z)$ is the Bessel function of the second kind and order μ (see Ref.¹⁶). For small argument the Bessel function can be approximated by formula¹⁶

$$K_\nu(z) \sim \frac{2^{\nu-1} \Gamma(\nu)}{z^\nu} \quad (35)$$

where $z \ll 1$. Using Eq.(35) it can be shown that for $qd \ll 1$ the ‘‘spring’’ model⁸ is valid for which $b = a = -K$, where K is a spring constant per unit area characterizing the interaction between the two solids⁸. At the equilibrium distance

$$a = -\frac{3\pi C_1}{d_0^5} = -K_0, \quad (36)$$

where K_0 is the spring constant at $d = d_0$. Thus the parameters of the interaction can be written in the form

$$a = \frac{K_0}{3} \left(\frac{d_0}{d} \right)^5 \left[2 - 5 \left(\frac{d_0}{d} \right)^6 \right], \quad (37)$$

$$b = \frac{q^3 d_0^5 K_0}{12d^2} \left[K_3(qd) - \frac{q^3 d_0^6 K_6(qd)}{192d^3} \right]. \quad (38)$$

2. Electrostatic interaction between dielectric surface and conducting 2D sheet

The electrostatic potential in the vacuum gap between the 2D sheet and dielectric has the form

$$\varphi = \sigma_g z + \text{const.} \quad (39)$$

The surface displacements of the sheet and dielectric

$$u_{zi}(\mathbf{x}) = u_i e^{i\mathbf{q} \cdot \mathbf{x}} \quad (40)$$

will give rise to normal component of surface dipole moments $p_{zi} = \sigma_i u_i$ resulting in a change of the electric field in the vacuum gap, which can be described by the potential

$$\phi(\mathbf{x}, z) = (\nu_- e^{-qz} + \nu_+ e^{qz}) e^{i\mathbf{q} \cdot \mathbf{x}}. \quad (41)$$

According to Eqs. (17)-(19), on the dielectric surface the boundary condition for the electric field takes the form

$$\nu_- e^{qd} = -R_{d0} \nu_+ e^{-qd} - 4\pi \sigma_g u_d R_{d0}, \quad (42)$$

where R_{d0} is determined by (23) at $\omega = 0$. In the electrostatic limit, the sheet potential should remain unchanged when the surface is displaced, from which follows the boundary condition¹⁰

$$4\pi \sigma_g u_g + \nu_- + \nu_+ = 0. \quad (43)$$

This Eq. (43) also can be obtained from (42) with $R_{d0} = 1$, $d = 0$ and changing u_d to u_g .

From (43) and (42)

$$\nu_+ = \frac{E_0}{1 - e^{-2qd} R_{d0}} (e^{-qd} R_{d0} u_d - u_g), \quad (44)$$

$$\nu_- = \frac{e^{-qd} R_{d0} E_0}{1 - e^{-2qd} R_{d0}} (e^{-qd} u_g - u_d). \quad (45)$$

The electric field normal to the surfaces of the 2D sheet and dielectric for $-d < z < 0$ is

$$E_z = -E_0 + \frac{qE_0}{1 - e^{-2qd} R_{d0}^0} [(e^{qz} + e^{-2qd} R_{d0} e^{-qz}) u_g - e^{-qd} (e^{qz} + e^{-qz}) R_{d0} u_d] e^{\mathbf{q} \cdot \mathbf{x}}, \quad (46)$$

and from Maxwell stress tensor, the stresses that act on the surfaces of the sheet and dielectric due to the surface displacements are

$$\sigma_g = K_g u_g - K u_d, \quad (47)$$

$$\sigma_d = K_g u_d - K u_g, \quad (48)$$

where

$$K_g = \frac{E_0^2 q (1 + e^{-2qd} R_{d0})}{4\pi (1 - e^{-2qd} R_{d0})}, \quad (49)$$

$$K_d = \frac{E_0^2 q R_{d0} (1 + e^{-2qd})}{4\pi (1 - e^{-2qd} R_{d0})}, \quad (50)$$

$$K = \frac{E_0^2 q e^{-qd} R_{d0}}{2\pi (1 - e^{-2qd} R_{d0})}. \quad (51)$$

3. Phonon heat flux between surfaces

The displacements of the surfaces $u_i = u_i^f + u_i^{ind}$, where u_i^f is the fluctuating displacement due to thermal and quantum fluctuations inside the bodies and u_i^{ind} is the induced displacement, which occurs due to the interaction between surfaces. Thus, according to Eqs. (29), (30), (47) and (48) the displacements of the surfaces are determined by

$$u_g = u_g^f + M_g \sigma_g = u_g^f + M_g (K_g u_g - K u_d), \quad (52)$$

$$u_d = u_d^f + M_d \sigma_d = u_d^f + M_d (K_d u_d - K u_g), \quad (53)$$

where M_i is the mechanical susceptibility which determines the surface displacement under an action of the applied stress: $u_i^{ind} = M_i \sigma_i$, and where

$$K_g = \frac{E_0^2 q (1 + e^{-2qd} R_{d0})}{4\pi (1 - e^{-2qd} R_{d0})} + \frac{K_0}{3} \left(\frac{d_0}{d} \right)^5 \left[2 - 5 \left(\frac{d_0}{d} \right)^6 \right], \quad (54)$$

$$K_d = \frac{E_0^2 q R_{d0} (1 + e^{-2qd})}{4\pi (1 - e^{-2qd} R_{d0})} + \frac{K_0}{3} \left(\frac{d_0}{d}\right)^5 \left[2 - 5 \left(\frac{d_0}{d}\right)^6 \right], \quad (55)$$

$$K = \frac{E_0^2 q e^{-qd} R_{d0}}{2\pi (1 - e^{-2qd} R_{d0})} + \frac{q^3 d_0^5 K_0}{12d^2} \left[K_3(qd) - \frac{q^3 d_0^6 K_6(qd)}{192d^3} \right]. \quad (56)$$

According to the fluctuation-dissipation theorem, the spectral density of fluctuations of the surface displacements is determined by¹⁷

$$\langle |u_{g(d)}^f|^2 \rangle = \hbar \text{Im} M_{g(d)}(\omega, q) \coth \frac{\hbar\omega}{2k_B T_{g(d)}}. \quad (57)$$

From (52) and (53)

$$u_g = \frac{(1 - M_d K_d) u_g^f - M_g K u_d^f}{(1 - M_g K_g)(1 - M_d K_d) - K^2 M_g M_d}, \quad (58)$$

u_d is obtained from u_g by the permutation of indexes ($g \leftrightarrow d$). The mechanical stress that acts on the surface of the dielectric, due to fluctuations of the surface displacement of the sheet, is determined by

$$\sigma_{dg}^f = \frac{K u_g^f}{(1 - M_g K_g)(1 - M_d K_d) - K^2 M_g M_d}. \quad (59)$$

The stress σ_{gd}^f can be obtained from σ_{dg}^f by the permutation ($g \leftrightarrow d$). The heat flux from the sheet to dielectric due to the electrostatic and van der Waals interactions between the fluctuating surface displacements is^{9,17}

$$\begin{aligned} J^{ph} &= \langle \dot{u}_d^{ind} \sigma_{dg}^f \rangle - \langle \dot{u}_g^{ind} \sigma_{gd}^f \rangle = 2 \int_0^\infty \frac{d\omega}{2\pi} \int \frac{d^2q}{(2\pi)^2} \omega \left[\text{Im} M_d \langle |\sigma_{dg}^f|^2 \rangle - \text{Im} M_g \langle |\sigma_{gd}^f|^2 \rangle \right] = \\ &= \frac{1}{\pi^2} \int_0^\infty d\omega [\Pi_g(\omega) - \Pi_d(\omega)] \int_0^\infty dq q \frac{K^2 \text{Im} M_g \text{Im} M_d}{|(1 - K_g M_g)(1 - K_d M_d) - K^2 M_g M_d|^2}. \end{aligned} \quad (60)$$

In the ‘‘spring’’ model⁸ it is assumed that $K_g = K_d = -K$ and in this case (60) is reduced to

$$J_{spr}^{ph} = \frac{1}{\pi^2} \int_0^\infty d\omega [\Pi_g(\omega) - \Pi_d(\omega)] \int_0^\infty dq q \frac{K^2 \text{Im} M_g \text{Im} M_d}{|1 + K(M_g + M_d)|^2}. \quad (61)$$

III. NUMERICAL RESULTS FOR GRAPHENE ON A SiO_2 SUBSTRATE

For an elastic sheet¹⁸

$$M_g = \frac{1}{\kappa q^4 - \rho \omega^2 - i\omega \rho \gamma}, \quad (62)$$

where the bending stiffness of graphene $\kappa \approx 1\text{eV}$, $\rho = 7.7 \cdot 10^{-7} \text{kg/m}^2$ is the surface mass density of graphene, γ is the damping constant for flexural motion of graphene which was estimated in Ref.¹⁹ as

$$\gamma = \frac{\omega T}{100 T_{RT}} \quad (63)$$

where $T_{RT} = 300\text{K}$ is the room temperature.

For an elastic semi-infinite medium the mechanical susceptibility M_d is determined by formula²⁰

$$M_d = \frac{i}{\rho c_t^2} \left(\frac{\omega}{c_t}\right)^2 \frac{p_l(q, \omega)}{S(q, \omega)}, \quad (64)$$

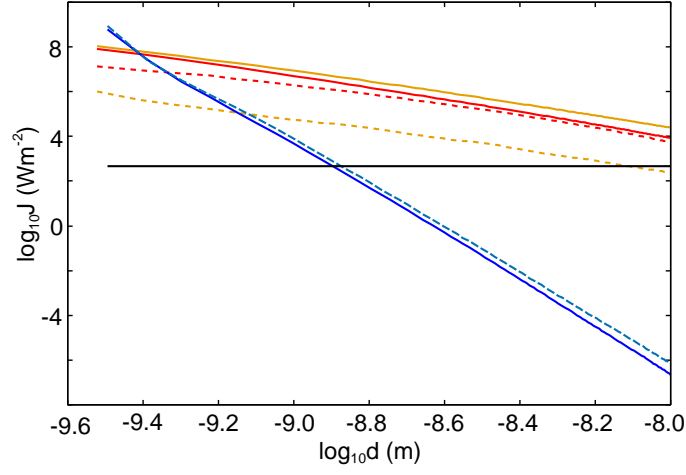


FIG. 1: Dependence of the heat flux between graphene and a SiO₂ substrate on the separation between them for different mechanisms. The red and brown lines show the heat flux for the radiative and electrostatic phonon heat transfer: the solid and dashed lines for the concentration of the free charge carries in graphene $n_g = 10^{19}\text{m}^{-2}$ and $n_g = 10^{18}\text{m}^{-2}$, respectively. The blue lines show the heat flux associated with the van der Waals interaction: the solid and dashed lines are for the nonlocal and local (the “spring” model) theories of the van der Waals phonon heat transfer. The black line shows the radiative heat transfer associated with blackbody radiation.

where

$$S(q, \omega) = \left[\left(\frac{\omega}{c_t} \right)^2 - 2q^2 \right]^2 + 4q^2 p_t p_l,$$

$$p_t = \left[\left(\frac{\omega}{c_t} \right)^2 - q^2 + i0 \right]^{1/2}, \quad p_l = \left[\left(\frac{\omega}{c_l} \right)^2 - q^2 + i0 \right]^{1/2},$$

where for SiO₂ the density $\rho = 2.65 \cdot 10^3 \text{kg/m}^3$, $c_l = 5968 \text{m/s}$ and $c_t = 3764 \text{m/s}$ are the longitudinal and transverse velocities of the acoustic waves.

The dielectric function of amorphous SiO₂ can be described using an oscillator model²¹

$$\varepsilon(\omega) = \epsilon_\infty + \sum_{j=1}^2 \frac{\sigma_j}{\omega_{0,j}^2 - \omega^2 - i\omega\gamma_j}, \quad (65)$$

where parameters $\omega_{0,j}$, γ_j and σ_j were obtained by fitting the measured ε for SiO₂ to the above equation, and are given by $\epsilon_\infty = 2.0014$, $\sigma_1 = 4.4767 \times 10^{27} \text{s}^{-2}$, $\omega_{0,1} = 8.6732 \times 10^{13} \text{s}^{-1}$, $\gamma_1 = 3.3026 \times 10^{12} \text{s}^{-1}$, $\sigma_2 = 2.3584 \times 10^{28} \text{s}^{-2}$, $\omega_{0,2} = 2.0219 \times 10^{14} \text{s}^{-1}$, and $\gamma_2 = 8.3983 \times 10^{12} \text{s}^{-1}$.

In the numerical calculations we used the dielectric function of graphene, which was calculated within the random-phase approximation (RPA)^{22,23}. The dielectric function is an analytical function in the upper half-space of the complex ω -plane:

$$\varepsilon_g(\omega, q) = 1 + \frac{4k_F e^2}{\hbar v_F q} - \frac{e^2 q}{2\hbar \sqrt{\omega^2 - v_F^2 q^2}} \left\{ G\left(\frac{\omega + 2v_F k_F}{v_F q}\right) - G\left(\frac{\omega - 2v_F k_F}{v_F q}\right) - i\pi \right\}, \quad (66)$$

where

$$G(x) = x\sqrt{x^2 - 1} - \ln(x + \sqrt{x^2 - 1}), \quad (67)$$

where the Fermi wave vector $k_F = (\pi n)^{1/2}$, n is the concentration of charge carriers, the Fermi energy $\epsilon_F = \hbar v_F k_F$, $v_F \approx 10^6 \text{m/s}$ is the Fermi velocity.

For graphene on a SiO₂ substrate at equilibrium distance, according to functional theory calculation, the spring constants¹⁹ $K_0 = K_{OH} = 1.23 \cdot 10^{20} \text{N/m}^3$ and $K_0 = K_H = 1.56 \cdot 10^{20} \text{N/m}^3$ for the OH- and H-terminated SiO₂ substrate, which agrees rather well with estimation $K_0 = 1.82 \cdot 10^{20} \text{N/m}^3$ in Ref.⁸

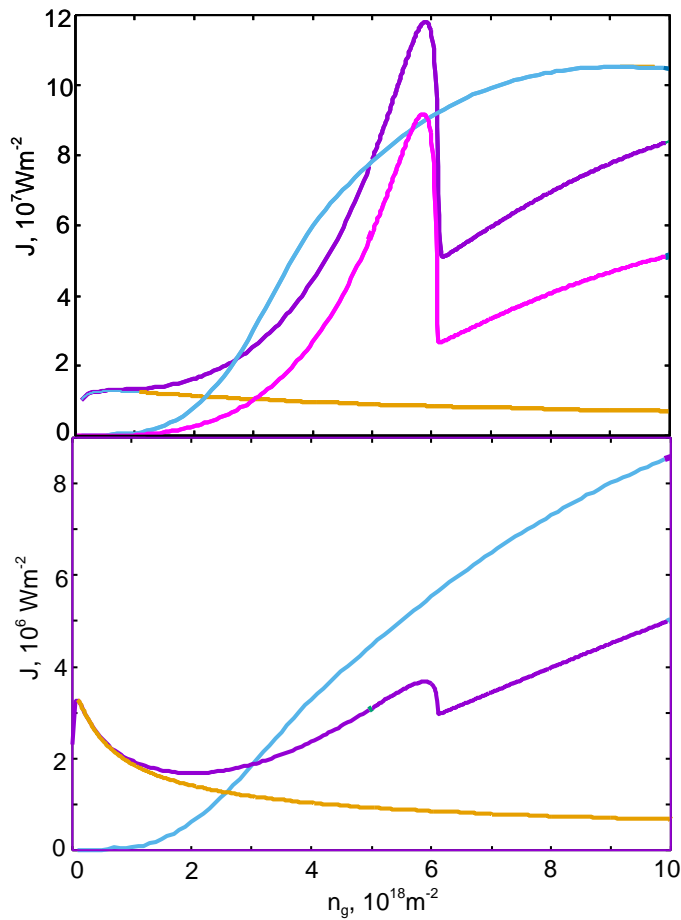


FIG. 2: Dependence of the heat flux between graphene and a SiO_2 substrate on the concentration of the free charge carries in graphene. The violet and blue lines show the radiative and electrostatic phonon heat flux at $d = 0.3\text{nm}$ (top) and $d = 1\text{nm}$ (bottom). The brown lines show the radiative heat flux without contribution from the thermally fluctuating surface displacements, while the pink line on the top shows only these contributions.

Fig. 1 shows the dependence of the heat flux between graphene and a SiO_2 substrate on the separation between them for different mechanisms and different free charge carries concentration n . The heat fluxes associated with the radiative and electrostatic phonon heat transfer have practically the same distance dependence and the difference between them decreases when the concentration n increases. The heat flux associated with the van der Waals interaction decays with distance much faster than for the radiative and electrostatic phonon heat transfer. Thus for $n_g > 10^{19}\text{m}^{-2}$ the radiative and electrostatic phonon heat transfer dominate for practically all separations. The blue solid and dashed lines show the contributions to the heat flux calculated using nonlocal and local theories of the van der Waals phonon heat transfer. For distances $d < 10\text{nm}$ the difference between these contributions is small, which confirms the validity of the “spring” model for such distances.

Fig. 2 shows the dependence of the heat flux associated with the radiative and electrostatic phonon heat transfer between graphene and a SiO_2 substrate on the concentration n_g at $d = 0.3\text{nm}$ (top) and $d = 1\text{nm}$ (bottom). For the radiative heat transfer, for $n_g > 10^{18}\text{m}^{-2}$ dominates the contribution which is associated with flexural vibrational modes of graphene. The sharp maximum in the radiative heat flux at $d = 0.3\text{nm}$ and $n_g \approx 6 \cdot 10^{18}\text{m}^{-2}$ is related with the phonon polariton resonance which occurs due to interaction of the flexural mode with an electric field of the charged sheet. The reflection amplitude for graphene at this resonance is determined by (16).

IV. CONCLUSION

The heat transfer between a 2D sheet and dielectric in presence of the gate voltage was calculated. The gate voltage induces a surface charge density on the of the sheet and dielectric. As a result, thermal fluctuations of

the surface displacements create a fluctuating electromagnetic field that leads to an additional contribution to the radiative heat transfer. The phonon heat transfer due to the electrostatic and van der Waals interactions between surface displacements was calculated taking into account the nonlocality of these interactions. Numerical results are presented for the heat transfer between graphene and a SiO₂ substrate. It has been shown that, when the charge density $\sigma_g > 0.1 \text{K}\mu\text{m}^{-2}$ is induced on the graphene surface, the main contribution to the radiative heat transfer is associated with the flexural vibrational modes of graphene, and this contribution is of the same order and has the same distance dependence as the contribution from the electrostatic phonon heat transfer. Due to the strong distance dependence the van der Waals phonon heat transfer is only important for subnanometer distances. For $\sigma_g > 1 \text{K}\mu\text{m}^{-2}$ the heat flux due to the radiative and electrostatic phonon heat transfer dominate for practically all distances. The obtained results can be important for the heat managements in the 2D devices.

A.I.V. acknowledges funding by RFBR according to the research project N^o 19-02-00453. A.I.V. also thanks the Condensed Matter group of ICTP for hospitality during the time of working on this article.

*alevolokitin@yandex.ru

-
- ¹ B. Li, L. Wang and G. Casati, Negative differential thermal resistance and thermal transistor, *Appl. Phys. Lett.* **88**, 143501 (2006).
 - ² N. Li, J. Ren, L. Wang G. Zhang, P. Hnggi, and B. Li, Phononics: Manipulating heat flow with electronic analogs and beyond, *Rev. Mod. Phys.* **84**, 1045 (2012).
 - ³ L. Wang, B. Li, Thermal logic gates: Computation with phonons, *Phys. Rev. Lett.* **99**, 177208 (2007).
 - ⁴ P. Ben-Abdallah and S.-A. Biehs, Near-field thermal transistor, *Phys. Rev. Lett.* **112**, 044301 (2014).
 - ⁵ P. Ben-Abdallah and S.-A. Biehs, Phase-change radiative thermal diode, *Appl. Phys. Lett.* **103**, 191907 (2013).
 - ⁶ K. Joulain, Y. Ezzahri, J. Drvillon, and P. Ben- Abdallah, Modulation and amplification of radiative far field heat transfer: Towards a simple radiative thermal transistor, *Appl. Phys. Lett.* **106**, 133505 (2015).
 - ⁷ K. S. Novoselov, A. K. Geim, S. V. Morozov, D. Jiang, Y. Zhang, S. V. Dubonos, I. V. Grigorieva, A. A. Firsov, Electric Field Effect in Atomically Thin Carbon Films, *Science*, **306**, 666 (2004).
 - ⁸ B.N.J. Persson, A.I. Volokitin and H. Ueba, Phononic heat transfer across an interface: thermal boundary resistance *J. Phys.: Condens. Matter* **23**, 045009 (2011).
 - ⁹ A.I. Volokitin, Effect of an Electric Field in the Heat Transfer between Metals in the Extreme Near Field, *JETP Lett.*, **109**, 749(2019).
 - ¹⁰ J.B. Pendry, K. Sasiithlu, R.V. Craste, Phonon-assisted heat transfer between vacuum-separated surfaces, *Phys. Rev. B* **94**, 075414 (2016).
 - ¹¹ A. Das, S. Pisana, B. Chakraborty, S. Piscanec, S.K. Saha, U.V. Waghmare, K.S. Novoselov, H.R. Krishnamurthy, A.K. Geim, A.C. Ferrari and A.K. Sood, Monitoring dopants by Raman scattering in an electrochemically top-gated graphene transistor, *Nature Nanotechnology*, **3**,210(2008).
 - ¹² A.I. Volokitin and B.N.J. Persson, Radiative heat transfer between nanostructures, *Phys. Rev. B* **63**, 205404 (2001).
 - ¹³ A.I. Volokitin and B.N.J. Persson, Near field radiative heat transfer and noncontact friction, *Rev.Mod.Phys.* **79**, 1291 (2007).
 - ¹⁴ A.I.Volokitin and B.N.J.Persson, *Electromagnetic Fluctuations at the Nanoscale. Theory and Applications*, (Springer, Heidelberg, 2017).
 - ¹⁵ D. C. Langreth, Macroscopic approach to the theory of reflectivity, *Phys. Rev. B*, **39**, 10020(1989).
 - ¹⁶ M. Abramowitz and I.A. Stegun, *Handbook of Mathematical Functions* (Dover 1970).
 - ¹⁷ L.D. Landau and E.M. Lifshitz, *Statistical Physics (Volume 5 of A Course of Theoretical Physics)* Pergamon Press 1980.
 - ¹⁸ L.D. Landau and E.M. Lifshitz, *Theory of Elasticity (Volume 7 of A Course of Theoretical Physics)* Pergamon Press 1970.
 - ¹⁹ Z.-Y. Ong, Y. Cai, and G. Zhang, Theory of substrate-directed heat dissipation for single-layer graphene and other two-dimensional crystals, *Phys. Rev. B* **94**, 165427 (2016).
 - ²⁰ B.N.J. Persson, Theory of rubber friction and contact mechanics *J. Chem. Phys.* **115**, 3840 (2001).
 - ²¹ D.Z.A. Chen, R. Hamam, M. Soljagic, J.D. Joannopoulos and G. Chen, Extraordinary optical transmission through sub-wavelength holes in a polaritonic silicon dioxide film, *Appl. Phys. Lett.* **90**, 181921 (2007).
 - ²² B. Wunscvh, T. Stauber, F. Sols, and F. Guinea, Dynamical polarization of graphene at finite doping, *New J.Phys.* **8**,318 (2006).
 - ²³ E.H. Hwang, S.Das Sarma, Dielectric function, screening, and plasmons in two-dimentional graphene, *Phys. Rev. B* **75**, 205418 (2007).